Materials and Structures (2023) 56:60
https://doi.org/10.1617/s11527-023-02148-2

ORIGINAL ARTICLE

On the role of compaction in disputes over the quality of the supplied concrete

André Valente Monteiro · Arlindo Gonçalves · Jean-Paul Balayssac · Marie-Pierre Yssorche-Cubaynes · António Costa

Received: 19 July 2022 / Accepted: 7 March 2023 / Published online: 24 March 2023

Abstract This paper evaluates the effect of poor compaction on the compressive strength, sorptivity, gas permeability and accelerated carbonation resistance of bulk concrete in structures, framed in the scenario of disputes over the quality of the supplied concrete. For that purpose, several real-scale elements (beams, columns and slabs) were cast with concrete incorporating Portland-limestone cement and fly ash addition, covering a wide range of slumps (35–123 mm) and compressive strengths (25–65 MPa). The elements were then subjected to different compaction conditions (standard vibration and no vibration), and later cored for concrete testing. A new compaction indicator that overcomes the main practical limitations associated with the determination of the excess voidage of concrete is proposed, as well as new factors for correcting the effects of on-site compaction in the estimation of the potential carbonation resistance and the compressive strength of concrete. It is also shown that vibration no longer improves the quality of bulk concrete in structures for slumps above $\sim$ 140 mm, which suggests that, in cases of dispute where greater slumps are specified, no correction for compaction should be needed in the estimation of the potential properties of concrete.

Keywords Vibration · Workability · Durability · Compressive strength · Carbonation · Porosity

A. Valente Monteiro (✉) · A. Gonçalves
National Laboratory for Civil Engineering, Avenida do Brasil, 101, 1700-066 Lisbon, Portugal
e-mail: avmonteiro@lnec.pt

A. Gonçalves
e-mail: arlindo@lnec.pt

J.-P. Balayssac · M.-P. Yssorche-Cubaynes
LMDC, Université de Toulouse, INSA, UPS Génie Civil, 135 Avenue de Rangueil, 31077 Toulouse Cedex 04, France
e-mail: balayssa@insa-toulouse.fr

M.-P. Yssorche-Cubaynes
e-mail: marie-pierre.cubaynes@iut-tlse3.fr

A. Costa
CERIS, IST-ID, Universidade de Lisboa, Av. Rovisco Pais, 1049-001 Lisbon, Portugal
e-mail: antonio.silva.costa@tecnico.ulisboa.pt

1 Introduction

Concrete in structures is often subjected to compaction conditions poorer than those of standard concrete specimens manufactured for prequalification and quality control purposes. This may occur due to several factors, such as, for example:

- The larger dimensions and often lower rigidity of the forms compared to standard moulds, which may reduce the effectiveness of vibration;
- The narrow on-site spaces to be filled (e.g. between the reinforcement and the forms), which may filter concrete constituents, leaving voids and creating

barriers that make it difficult for trapped air to escape during vibration;
- Differences in concrete rheological properties resulting, for example, from variations in mix proportions and concrete temperature during production and placement, as well as from delays in the transportation of concrete to the worksite.

Poor compaction increases concrete porosity and can significantly impair both the mechanical [1–3] and the durability-related [4–7] performance of concrete, as well as the bond strength of embedded reinforcement [3, 8]. Knowledge of the magnitude of the effects of on-site compaction on concrete quality is crucial not just to promote an adequate mix design and execution of concrete structures, but also to make fair decisions (e.g. assignment of liabilities) in cases of dispute over the quality of the supplied concrete (e.g. when conformity based on standard control specimens is in doubt). In practice, concrete specification has been traditionally based on prescriptive methods, in which limits are established for the composition and the compressive strength of concrete, and where quality control is essentially based on controlling its compressive strength during execution. Consequently, disputes over the quality of the supplied concrete are generally resolved on the basis of the assessment of concrete compressive strength, for which guidelines can be found in technical documents [9] and standards [10, 11]. Today, with the increased use of new binders in concrete, there is a growing trend towards the performance-based specification of concrete durability [12], in which the prescriptive limits to the composition of concrete are replaced by limits to its durability-related properties (e.g. carbonation resistance and resistance to chloride penetration). The transition to the performance-based specification of concrete durability has been a slow process, which basically started with the incorporation of service-life models in international codes [13] and standards [14], as well as in national regulations [15, 16]. More recently, CEN has decided to take a large step towards this transition, by planning the incorporation of Exposure Resistance Classes in the next version of Eurocode 2, which will be addressed in a new part of the European Standard EN 206, in relation to carbonation- and chloride-corrosion. Therefore, it is expected that future disputes over the quality of the supplied concrete will also be focused on the assessment of the durability-related properties of concrete. However, no guidelines can be found in the literature to perform such assessment.

Disputes resolved on the basis of the assessment of compressive strength usually involve drilling cores from the structure and estimating the potential compressive strength of concrete (i.e. as if it was manufactured, cured and tested as the standard control specimens), f_c, using factors to correct the effects associated with execution and testing conditions, as follows:

$$f_c = C_{\mathrm{Comp.}} \times C_{\mathrm{Curing}} \times C_{\mathrm{Age}} \times C_{\mathrm{Dir.}} \times C_D \times C_{L/D} \times C_{\mathrm{RH}} \times \ldots \times f_{\mathrm{c,is}} \tag{1}$$

where

- $f_{\mathrm{c,is}}$ is the core compressive strength;
- $C_{\mathrm{Comp.}}$ and C_{Curing} are strength correction factors that account for on-site compaction and curing conditions of concrete, respectively;
- C_{Age}, $C_{\mathrm{Dir.}}$, C_D, $C_{L/D}$, C_{RH}, … are strength correction factors that account for the effects of core testing conditions, such as, respectively: age of testing; direction of drilling; diameter, length-to-diameter ratio and internal relative humidity of the cores; etc.

With respect to the effects of compaction in particular, values for the strength correction factor $C_{\mathrm{Comp.}}$ can be found in CSTR11 [9] and BS 6089 [11], as a function of the excess voidage of concrete resulting from imperfect compaction. This excess voidage can be determined in two ways: by means of density measurements on cores drilled from the structure, which need to be compared with the (potential) density of the standard control specimens; or by visual examination of the cores, comparing the number and size of the voids exposed on their surface with those displayed in reference images of concrete specimens of known actual voidage. In principle, a similar approach can be used for assessing the potential durability-related properties of concrete, using correction factors for compaction applicable to such properties. This methodology has, however, two long-known limitations associated with the determination of the excess voidage that need to be overcome:

- The density method can only be determined if the potential density of concrete is known. However, in practice, this information is not always available. It has also been pointed out that on-site curing conditions may affect the density of concrete, which may lead to biased estimates of its excess voidage [9];

- The visual method can only be performed in a discrete manner and is highly subjective, since it is based on an individual interpretation of what reference image best resembles the distribution of visible surface voids in the cores. In addition, this method depends on uncontrolled factors that may affect the examination of the cores, such as light conditions, colour of concrete constituents, etc.

This paper studies the effect of on-site compaction conditions on the compressive strength, sorptivity, gas permeability and accelerated carbonation resistance of concrete in structures. For that purpose, real-scale elements were cast with concrete made with and without fly ash addition, covering a wide range of slumps and compressive strengths. The elements were then subjected to different compaction conditions, and later cored for concrete testing. A new compaction indicator that overcomes the main practical limitations associated with the determination of the excess voidage is developed, as well as new correction factors for compaction applicable in cases of dispute over the carbonation resistance and the compressive strength of the supplied concrete.

2 Methods

2.1 Concrete composition and casting

Six concrete loads of 3 m^3 were produced by a local supplier, in a ready-mixed concrete plant, with the compositions and slumps described in Table 1. Two binders were used—Portland-limestone cement type CEM II/A-L 42.5 R [17], with and without a 30 wt.% replacement level of fly ash addition. All concrete mixtures had a maximum aggregate size of 25 mm. Table 2 shows the chemical composition and the physical properties of the cement and the fly ash used in the mixtures.

With each concrete load, two 0.50 × 0.50 × 2.00 m reinforced columns, a 0.40 × 0.50 × 2.00 m reinforced beam and a 0.20 × 1.50 × 3.00 m plain slab were cast outdoors, over a concrete floor (Fig. 1). The slabs were cast over a polyethylene sheet to prevent the absorption of water from concrete by the floor. In one of the columns and in two thirds of the length of the beams and slabs, the concrete was vibrated with a poker vibrator with a head diameter of 44 mm and a standard frequency (170 Hz, which meets the performance requirements recommended by ACI 309R-05 [18] for the internal vibration of concrete in these types of element), until the formation of air bubbles at the top surface of the elements practically ceased, as recommended by EN 13670 [19]. After vibration, the other column and the remaining length of the beam and slab were cast, and the concrete was just levelled at the top surface of the elements. In both columns, the maximum free-fall height of concrete was limited to 1.5 m to avoid any related adverse effect on concrete quality. Figure 2 describes the design details, as well as the compaction and curing conditions of the concrete elements (the reason for the different curing conditions is that this work was carried out as part of a wider research program that also addressed the effect of curing on concrete properties [20]).

2.2 Sampling and testing

Cores of 100 and 150 mm in diameter were drilled from the outdoor concrete elements at different concrete ages (four days before the age of testing) to determine the compressive strength, sorptivity, gas permeability and accelerated carbonation of both the vibrated and the non-vibrated concrete, as well as the excess voidage and the open coarse porosity of the non-vibrated concrete. The cores were cut according to Fig. 3 and immersed in water for at least 48 h before the testing age.

All the tests were performed on the concrete at a certain distance from the exposed surface of the elements (bulk concrete), so the wall effect and the effect of curing could be minimized. For each test, all specimens were cut from a different core so that the variability of the concrete quality within the element could be represented, as well as possible, by the test results. In the case of the columns, for each test, one specimen was cut from a core drilled from the upper, middle and lower third of the columns so that the variability of the concrete quality along their height could be evaluated. Table 3 shows the age of testing, as well as the number and dimensions of the cored specimens used in each test.

Table 1 Concrete composition and slump

Mix name	CEM II/A-L 42.5 R (kg/m^3)	Fly ash (kg/m^3)	Natural siliceous sand[a] (kg/m^3)	Crushed limestone coarse aggregate[a] (kg/m^3)	Admixture[b] (wt% of the binder)	Eff. w/b	Slump[c] (mm)
S0.65	240		930	1070	1.30 (P)	0.65	103
S0.50	340		820	1060	0.54 (P)	0.50	48
S0.35	440		750	1090	0.60 (P) + 0.60 (SP)	0.35	123
S0.65F	182	78	910	1020	0.70 (P)	0.65	35
S0.50F	238	102	810	1040	0.60 (P)	0.50	85
S0.40F	294	126	690	1100	0.70 (P)	0.40	105

[a]Saturated surface-dry. [b]P—Plast. Pozzolith 540; SP—Superplast. Glenium Sky 548. [c]Average of two slump test results

Table 2 Chemical composition (in wt%) and physical properties of the binders

	CEM II/A-L 42.5R	Fly ash
CaO	58.9	5.5
SiO_2	18.7	49.8
Al_2O_3	5.6	23.2
Fe_2O_3	3.1	7.8
SO_3	2.8	0.8
MgO	1.8	1.6
Na_2O	0.2	1.2
K_2O	1.0	1.8
Ins. Res	4.4	
LOI	7.1	5.8
Free CaO		0.6
Blaine [cm^2/g]	4050	4040
Density [kg/m^3]	3028	2350

The compressive strength was determined according to EN 12504-1 [21], with the end surfaces of the specimens being prepared by grinding. The remaining test methods are described below.

2.3 Accelerated carbonation resistance

Each specimen was sealed with aluminium foil in all surfaces but one of 140 × 150 mm (due to the presence of large voids, the uncut surface of the specimens with non-vibrated concrete needed to be previously sealed with melted paraffin wax). It was then exposed to the laboratory air conditions (20 ± 2 °C and 50 ± 10% r.h.) for 14 days and placed in a ventilated chamber at 23 ± 1 °C 60 ± 5% r.h. and 5.0 ± 0.1% CO_2 (0.09 kg of CO_2 per m^3 of air) in such a way that the air could circulate freely over the unsealed surface. Four periods of exposure were considered, which were well-spaced over 25 days (concrete S0.65 and 0.65F) or 36 days (concrete S0.50 and S0.50F). After each period, the specimen was removed from the chamber and transversally fractured (Fig. 3) and a concrete segment about 15 mm thick being obtained. The remaining specimen was immediately sealed with melted paraffin in its fractured surface and placed back in the carbonation chamber. The carbonation depth was measured on six points spaced by 15 mm, in the fractured surface of the concrete segment (between 50 and 125 mm away from the originally exposed surface of the element), using a phenolphthalein solution and a digital calliper, according to RILEM Recommendations [22]. The accelerated-carbonation resistance R_C of the specimen was determined by the following expression:

$$R_C = 2c/k_c^2 \quad [\text{kg year/m}^5] \tag{2}$$

where c is the CO_2 concentration of the air in the chamber (0.09 kg/m^3); and k_c is the coefficient of carbonation, which was estimated by linear regression analysis, using the following model and the four pairs of results (x_d^2,t):

$$x_d^2 = k_c^2 \cdot t \quad [\text{m}^2] \tag{3}$$

where x_d is the average carbonation depth of the test specimen after the exposure period t; and k_c^2 is the fitting parameter.

Fig. 1 Concrete elements

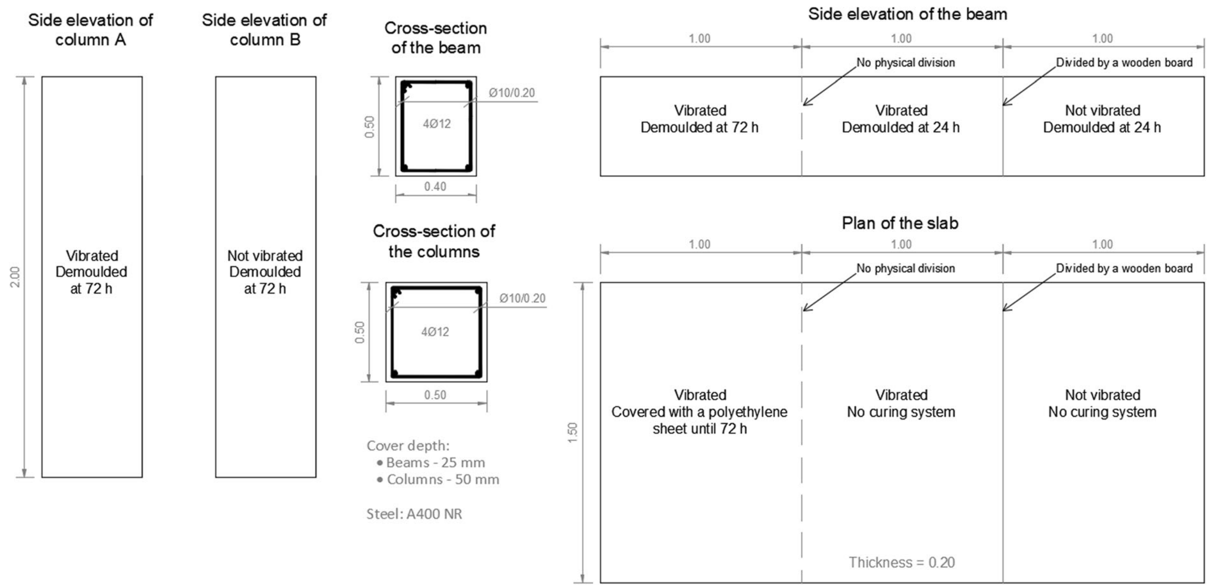

Fig. 2 Design details (in m), compaction and curing of each set of concrete elements

2.4 Water absorption and gas permeability

Each specimen was sealed with aluminium foil on its curved surface and dried for 3 days in a ventilated chamber at 50 ± 2 °C. Afterwards, the specimen was sealed with cellophane film, placed in a sealed plastic box and kept for 14 days in the ventilated chamber at 50 ± 2 °C, for moisture redistribution. After cooling down to 20 ± 1 °C for 24 h, the specimen was unwrapped and subjected to the gas permeability and water absorption tests according to RILEM Recommendations [23], using oxygen as the permeating gas, and with the uptake of water by capillary absorption being measured at 1, 2, 4 and 8 h. The apparent gas-permeability K_a (in $\times$ 10^{-16} m^2) was determined according to the RILEM-CEMBUREAU method [23]. The sorptivity S (in $\times$ 10^5 g mm^{-2} $h^{-0.5}$) of the specimen was determined by linear regression analysis, using the following model and the four pairs of results ($w(t)$,t):

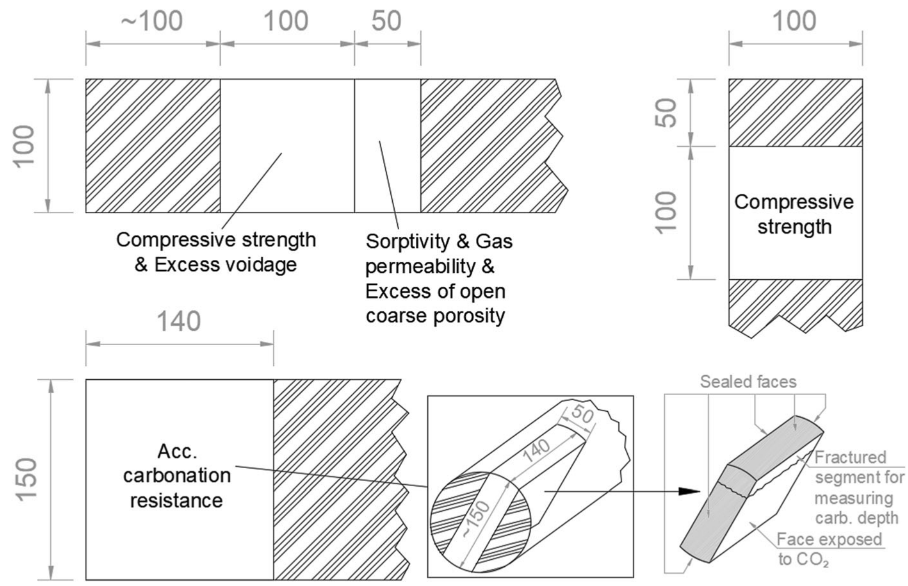

Fig. 3 Cutting scheme of the test specimens (dimensions in mm)

Table 3 Testing program

Elements	Age of testing[(1)] (days)	Number of test specimens per compaction condition		
		Compressive strength (f_c) & Excess voidage	Sorptivity (S) & Gas perm. & Excess of open coarse porosity	Acc. carbonation resistance[(2)] (R_c)
Beams (Vib. demoulded at 72 h & Non-vib.)	28	3	3	2
	91	3		
Columns (Vib. & Non-vib.)	91	3	3	3
Slabs (Vib. no curing system & Non-vib.)	91	3		
	364	3		
Specimen dimensions (mm)		100 × ϕ100	50 × ϕ100	50 × 140 × 150

[(1)] For the 50 × ϕ100 mm and 50 × 140 × 150 mm specimens, the age of testing corresponds to the concrete age at the time when the preconditioning procedure was initiated

[(2)] Only concrete S0.65, S0.65F, S0.50 and S0.50F

$$w(t) = A + S \cdot \sqrt{t} \quad [\times 10^5 \mathrm{g/mm^2}] \tag{4}$$

where $w(t)$ is the mass of water absorbed per unit area of the surface of the test specimens in contact with water at the suction period t.; and A and S are the fitting parameters.

It should be noted that, since the relative humidity in the ventilated chamber could not be controlled, the specimens from the same concrete mix were all dried at the same time to ensure, as well as possible, that they were exposed to the same hygrometric conditions.

2.5 Excess voidage

The excess voidage of non-vibrated concrete was determined on the basis of the apparent density of the water-soaked specimens, immediately before the compressive test, using the following expression[1]:

$$\text{Excess voidage} = \frac{D_{\text{vib}} - D_{\text{no vib}}}{D_{\text{vib}} - k \times \rho} \times 100\% \quad [\text{vol\%}] \tag{5}$$

where D_{vib} and $D_{\text{no vib}}$ are the saturated densities of vibrated and non-vibrated concrete, respectively, determined according to EN 12390–7 [24], with the volume obtained by measurement of the actual dimensions; k is the fraction of the voids in the specimen with non-vibrated concrete resulting from imperfect compaction and filled with water when $D_{\text{no vib}}$ is measured (taken as 0.5, as recommended by CSTR11 [9]; and ρ is the water density (1000 kg/m^3). Expression (5) is adopted from CSTR11 [9], with the sole difference of the concrete density being determined by the measurement of the actual dimensions of the specimens rather than by the water displacement method, to take into account, to some extent, the volume of the superficial voids of the specimens.

2.6 Excess of open coarse porosity

The excess of open coarse porosity of non-vibrated concrete was determined on the basis of the water-soaked and vacuum-saturated masses of the specimens used in the water absorption test, as follows [20]:

$$\text{Excess of open coarse porosity} = p_{\text{oc, no vib}} - p_{\text{oc, vib}} \quad [\text{vol\%}] \tag{6}$$

where $p_{\text{oc,vib}}$ and $p_{\text{oc,no vib}}$ are the open coarse porosities of vibrated and non-vibrated specimens, respectively, which are determined by the following expression:

$$p_{\text{oc}} = \frac{m_{\text{vac}} - m_{\text{cap}}}{\rho \times V} \times 100\% \quad [\text{vol\%}] \tag{7}$$

where m_{cap} is the mass of the water-soaked specimens; m_{vac} is the mass of vacuum-saturated specimens; V is the volume of the specimens determined by measurement of the actual dimensions; and ρ is the water density (1000 kg/m^3). The vacuum saturation procedure consisted of placing the specimens in a reservoir in a vacuum chamber at an absolute pressure below 50 mbar and 21 $\pm$ 4 °C. After 24 h, water was slowly introduced in the reservoir, until full immersion of the specimens, keeping the pressure below 50 mbar. After another 24 h, the atmospheric pressure was re-established in the chamber and the specimens were kept immerged in water for further 24 h. The specimens were then removed from the water reservoir, wiped with a wet cloth to remove the excess water from its surfaces and weighed.

The open coarse porosity parameter was developed aiming to find a compaction indicator that could be determined in an objective manner without knowing the potential density of concrete. It is known that poor compaction results in an excessive volume of pores caused by entrapped air that is accidentally introduced in concrete during mixing and pouring. Some of these pores are typically much larger than those usually found in fully-compacted concrete and have very low capillary suction potential. Hence, the difference between the total open porosity (measured in vacuum-saturated specimens) and the open porosity able of absorbing water by capillarity (measured in water-soaked specimens, i.e. by immersion at atmospheric pressure) is expected to be a measure of the volume of those pores, providing an indication of the level of concrete compaction. However, in this study was observed that vibrated concrete also exhibits non-negligible open coarse porosities (which should be due to imperfect compaction), and, therefore, the compaction indicator of concrete had to be considered as the difference between the open coarse porosities of non-vibrated and vibrated concrete, i.e. the excess of open coarse porosity.

3 Results

A wide range of compressive strengths (25–65 MPa) and carbonation resistances (37–292 kg year/m^5) were obtained in this study. Tables 4 and 5 show the test results (average values) obtained on vibrated and non-vibrated concrete, respectively.

---

[1]
$$\frac{D_{vib} - D_{novib}}{D_{vib} - k \times \rho} = \left(1 + \frac{k \times \rho - D_{novib}}{D_{vib} - k \times \rho}\right) = \left(1 + \frac{\frac{k\times\rho\times\left(V_s+V_p+\Delta V_p\right)-\left(m_s+m_w+k\times\rho\times\Delta V_p\right)}{V_s+V_p+\Delta V_p}}{\frac{m_s+m_w-k\times\rho\times\left(V_s+V_p\right)}{V_s+V_p}}\right) = \left(1-\frac{V_s+V_p}{V_s+V_p+\Delta V_p}\right) = \frac{\Delta V_p}{V_s+V_p+\Delta V_p} = \frac{\Delta V_p}{V_t}$$

where: $D_{vib} = \frac{m_s+m_w}{V_s+V_p}$; $D_{novib} = \frac{m_s+m_w+k\times\rho\times\Delta V_p}{V_s+V_p+\Delta V_p}$; m_s and m_w are the mass of solids and water in concrete; V_s and V_p are the solid and pores volumes in concrete, respectively; ΔV_p is the volume of pores resulting from imperfect compaction; and V_t is the total volume of the non-vibrated concrete.

4 Discussion

4.1 Beams and columns

4.1.1 Performance properties versus slump

The workability of conventional vibrated concrete, i.e. the ease of mixing, placing, compacting and finishing it to a homogeneous condition [25], is closely related to its rheological properties, in particular to its flow behaviour. There is a general agreement that its flow can be approximately described by the Bingham model [25], which depends on two rheological properties—the yield stress and the plastic viscosity. However, in practice, measuring these two properties on concrete can be expensive and time consuming [26], especially on site. For that reason, the slump test remains today the most universally used test to measure and control the workability of concrete, as it is simple and inexpensive. The slump is also intimately related to the yield stress of concrete (i.e. the minimum shear stress required to initiate flow) [25, 26], and is generally considered to be sufficient to control the workability of conventional vibrated concrete. Plastic viscosity has been considered to be most relevant for controlling the resistance to segregation and bleeding of highly-flowable concrete [27–29], although it has been found that it may also interfere with the migration of air bubbles in mortars [30].

Figure 4 shows the measured excess voidage and relative properties of non-vibrated concrete from the beams and columns as a function of slump. The error bars represent the corresponding relative value of the standard deviation of the test results of the non-vibrated concrete (i.e. average value ± standard deviation). The empty markers in Fig. 4f correspond to the gas permeability values obtained from the non-vibrated concrete where only a single specimen could be tested. Figure 4 clearly shows the impact of slump on the bulk properties of non-vibrated concrete, with the excess voidage surpassing 8 vol.% within the slump class S1, whereas the general trend suggests that vibration ceases to improve the quality of bulk concrete at the upper end of the slump class S3 (i.e. for slumps above ∼ 140 mm). This should not apply, however, to concrete cast near surfaces (e.g. near to forms or reinforcement), in which the volume of voids may increase significantly due to the absence of vibration, especially around reinforcing bars, as concrete struggles to completely infill the narrower spaces. In this study, even the concrete with the greatest slump exhibited that behaviour (Fig. 5). A good concrete compaction in those areas is crucial to ensure adequate durability and bond strength of reinforcement. Grampeix et al. [3] observed that vibration has a major beneficial impact on the bond strength of reinforcement for concrete with slumps as high as 180 mm. For concrete slumps above 210 ∼ 220 mm, this beneficial impact seems to no longer occur [3, 8].

The non-vibrated concrete from the columns shows, in general, a better quality compared to that from the beams. This seems to be related to the effect of the self-weight of non-vibrated concrete, as Fig. 6 shows, in which, unlike the vibrated concrete, the density of the non-vibrated concrete generally increases at the base of the columns.

4.1.2 Performance properties versus excess voidage

Figure 7 shows the relative properties of non-vibrated concrete as a function of excess voidage. In this figure, fly ash does not show any particular impact on the correlation between the measured performance properties and the excess voidage of concrete.

Several relationships have been proposed to relate the compressive strength with the porosity of cement-based materials, the most common ones being based on linear [31], exponential [32], logarithmic [33] and power [34] relationships. These models have later proved to be inadequate, which favoured the development of models that would also take into account the pore size distribution [35, 36] and, subsequently, the cement content [37]. However, the inadequacy of the models exclusively based on concrete porosity has apparently been only observed in cement-based materials with varied cement contents, types of aggregate and curing conditions, among other factors [37]. In fact, studies based on concrete with varied porosities, which were exclusively due to compaction or intentionally entrained air, have shown good strength-porosity correlations, by usually presenting strength reductions of about 5 to 6% per each 1 vol% of excess voidage, for excess voidages up to about 10% [1, 38]. In practice, relationships depending exclusively on porosity have been preferred by practitioners to resolve disputes over the quality of

Table 4 Properties of vibrated concrete

Mix name	f_c^{vib} (MPa)					R_c^{vib} (kg year/m^5) | K_a^{vib} ($\times$ 10^{-16} m^2)		S^{vib}($\times$ 10^5 g mm^{-2} h$^{-0.5}$) | $p_{oc, vib}$ (vol.%)	
	Beam 28 d	Beam 91 d	Column 91 d	Slab 91 d	Slab 364 d	Beam 28 d	Column 91 d	Beam 28 d	Column 91 d
S0.65	25	29	29	28	30	41|0.50	37|0.75	49|1.6	60|2.8
S0.50	48	52	53	51	55	292|0.05	260|0.09	21|1.8	27|1.4
S0.35	58	64	65	62	63			10|2.4	13|2.0
S0.65F	33	43	42	40	44	56|0.05	70|0.02	19|0.8	17|0.6
S0.50F	47	54	52	48	56	123|0.02	153|0.01	14|0.7	17|0.9
S0.40F	58	62	58	58	61			6|0.7	10|0.9

Table 5 Properties of non-vibrated concrete

Mix name	$f_c^{no\ vib}$(MPa) | Excess voidage (vol%)					$R_c^{no\ vib}$ (kg year/m^5) | $K_a^{no\ vib}$ ($\times$ 10^{-16} m^2)		$S^{no\ vib}$[$\times$ 10^5 g mm^{-2} h$^{-0.5}$] | $p_{oc,no\ vib}$ (vol%)	
	Beam 28 d	Beam 91 d	Column 91 d	Slab 91 d	Slab 364 d	Beam 28 d	Column 91 d	Beam 28 d	Column 91 d
S0.65	21|4.8	25|4.6	24|3.5	29|1.9	31|1.6	31|1.16	32|1.70	55|4.0	63|5.0
S0.50	35|5.8	37|5.9	40|4.6	55|2.6	62|1.8	143$^{(1)}$|0.18$^{(2)}$	226|0.21	32|4.9	36|4.1
S0.35	54|1.6	56|1.9	59|1.6	61|1.7	62|1.5			11|4.0	11|3.3
S0.65F	22|8.7	24|8.7	32|5.7	33|4.2	44|1.2	26|0.24$^{(2)}$	46|0.46$^{(2)}$	26|5.1	24|4.1
S0.50F	39|2.7	45|2.8	47|2.3	52|0.8	62|1.0	111|0.05	142|0.02	17|2.2	14|1.4
S0.40F	50|2.5	57|2.2	59|2.7	59|0.5	65|0.2			7|1.0	9|1.5

$^{(1)}$The carbonation depths measured during the tests showed a significant deviation from the function given by expression (3)

$^{(2)}$Only a single specimen could be properly tested as the permeability of the remaining specimens were above the reliable range of the permeameter

the supplied concrete. This has been in part motivated by the recommendations of CSTR11 [9] and BS 6089 [11], which provide factors to correct the effect of poor compaction on the compressive strength of concrete based on its excess voidage. More recently, Erkkilä et al. [39] studied the dependence of the compressive strength of mortars solely on porosity, based on simulations of the distribution of pores between 20 and 500 μm in size. They found a good correlation between the compressive strength and the cubic root of porosity, with the non-linearity of the results occurring mostly within the very low range of porosities (< 0.5 ~ 1.0 vol%). In the present study, still, the linear model showed a good fit to the measured compressive strengths within the range of the excess voidages obtained (Fig. 7a). The following expression was estimated by regression analysis, considering $f_c^{vib}/f_c^{no\ vib}$ as the dependent variable:

$$\frac{f_c^{vib}}{f_c^{no\ vib}} = 1/(1 - 4.51 \times \text{Excess voidage}) \tag{8}$$

with a standard error of estimate of 0.08 (i.e. the estimated standard deviation of residuals, which is an estimate of the standard deviation of $f_c^{vib}/f_c^{no\ vib}$). Table 6 shows the strength correction factors for compaction, $C_{Comp.}^{fc}$ (equivalent to $f_c^{vib}/f_c^{no\ vib}$), derived from expression (8). It should be noted that adopting a value for k other than 0.5 (i.e. when estimating the excess voidage by expression (5)) changes the slope of the denominator in expression (8), but practically does

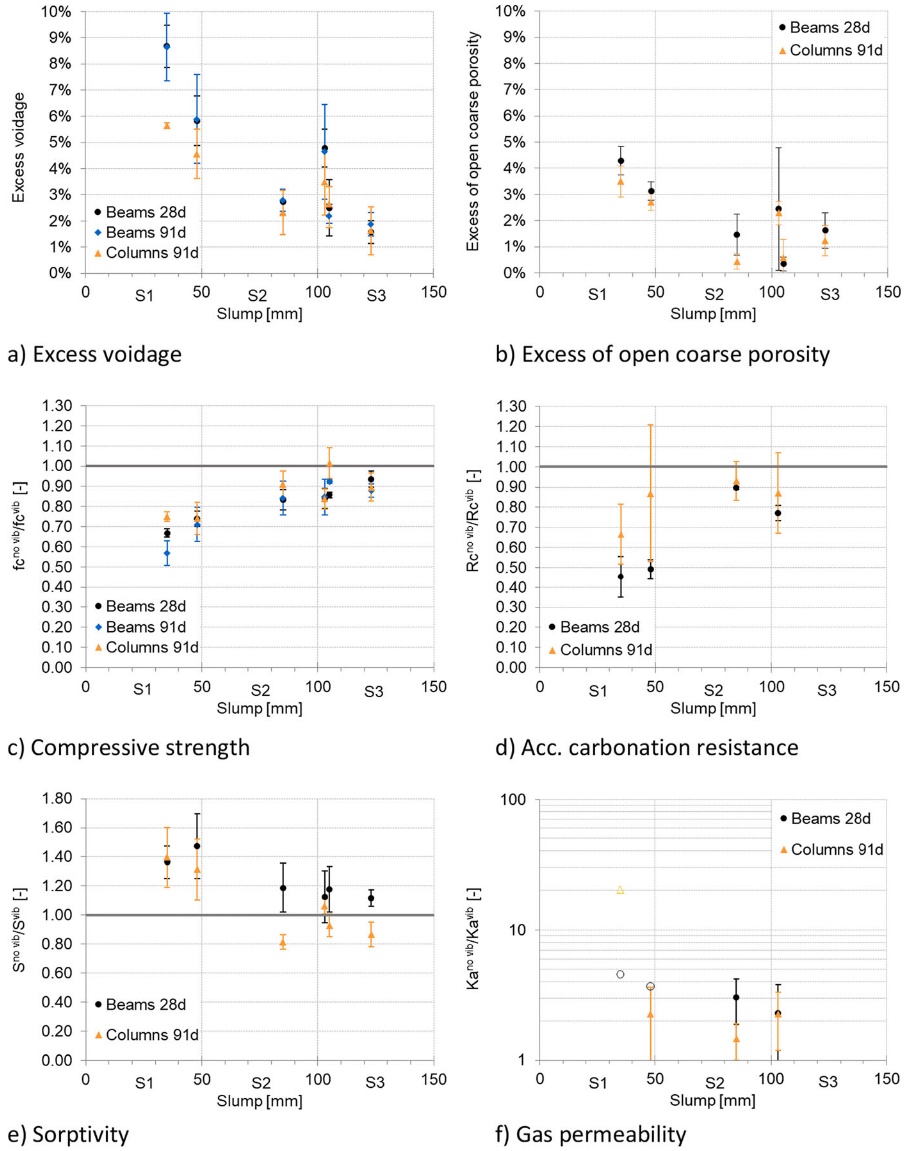

Fig. 4 Relative properties of non-vibrated concrete vs Slump (beams and columns)

not affect its goodness of fit. Expression (8) shows a good agreement with the correction factors recommended by BS 6089 [11], as shown in Fig. 7a. The correction factors recommended by CSTR11 [9], however, appear to follow the lower envelope of the results, and, therefore, they should be less suitable for resolving disputes over the quality of supplied concrete, in which the risks must be balanced between the contractor and the concrete producer.

The accelerated carbonation resistance (Fig. 7b) also seems to exhibit a good correlation with the excess voidage of concrete. The following relationship was estimated by regression analysis, considering $R_c^{\mathrm{vib}}/R_c^{\mathrm{no\ vib}}$ as the dependent variable:

$$\frac{R_c^{\mathrm{vib}}}{R_c^{\mathrm{no\ vib}}} = 1/\left(1 - 14.0 \times \text{Excess voidage}^{1.31}\right) \qquad (9)$$

with a standard error of estimate of 0.05. In this regression analysis, a potential outlier corresponding to the results obtained in the beam with concrete S0.50 was dismissed, since the carbonation depths measured during the tests exhibited a significant deviation from

Fig. 5 Compaction voids concentrated close to steel bars, at the surface of the non-vibrated column (concrete S0.35)

the function given by expression (3). Table 6 shows the correction factors for correcting the effect of compaction on the accelerated carbonation resistance of concrete, $C^{\mathrm{Rc}}_{\mathrm{Comp.}}$ (equivalent to $R_c^{\mathrm{vib}}/R_c^{\mathrm{no\ vib}}$), derived from expression (9). Due to the large uncertainty associated with measuring the carbonation depth in very poorly compacted concrete, the use of correction factors for excess voidages greater than 5% is not recommended. The scatter associated with expression (9) (observed in Fig. 7b) can partly result not only from the statistical uncertainty (associated with the small number of carbonation tests) but also from the variability in R_c associated with difficulties in measuring the carbonation front of non-vibrated concrete, which was not always sharp. Figure 8 shows the worst case observed during testing, in which the carbonation front is frequently disrupted due to large compaction voids. Another possible factor that may have contributed to the uncertainty of expression (9) may be related to the direction of the CO_2 ingress into the concrete specimens. Leemann et al. [40] found that vibration can lead to significant differences in the porosity of the lower, lateral and upper interfacial transition zones between the aggregates and the cement paste, with possible consequences for the transport properties of concrete. In addition, during vibration, there is the tendency for an upward movement of water inside concrete, which may create permeable paths after hardening. Arguably, these two factors could cause anisotropy in the transport properties of concrete. In the present study, however, the effect of a possible anisotropy was not evaluated since, due to the procedure adopted for cutting the specimens used in the carbonation tests (Fig. 3), the direction of CO_2 penetration into the specimens relative to the casting direction was not controlled.

Figure 7c does not exhibit a clear relationship between the sorptivity and the excess voidage. Since part of the voids resulting from poor compaction are too large to be able to absorb water during the water absorption test (i.e. due to their low capillary suction potential), some authors [41, 42] have suggested that water absorption may be lower when concrete is poorly compacted. The results obtained in this work suggest that it should only happen for very large excess voidages (i.e. for more poorly compacted concrete than those studied here), as values of S^{vib}/S^{novib} above one were generally obtained for excess voidages up to about 9 vol.%. Gonen and Yazicioglu [4] also observed increased sorptivities in poorly compacted concrete. This increase may result

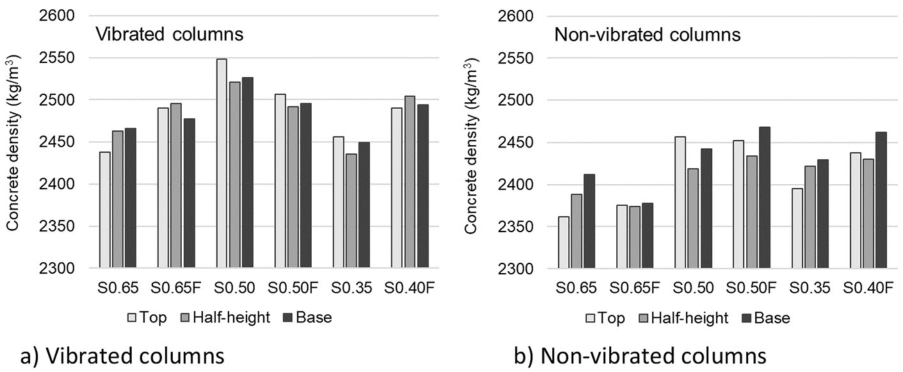

Fig. 6 Concrete density along the height of the columns

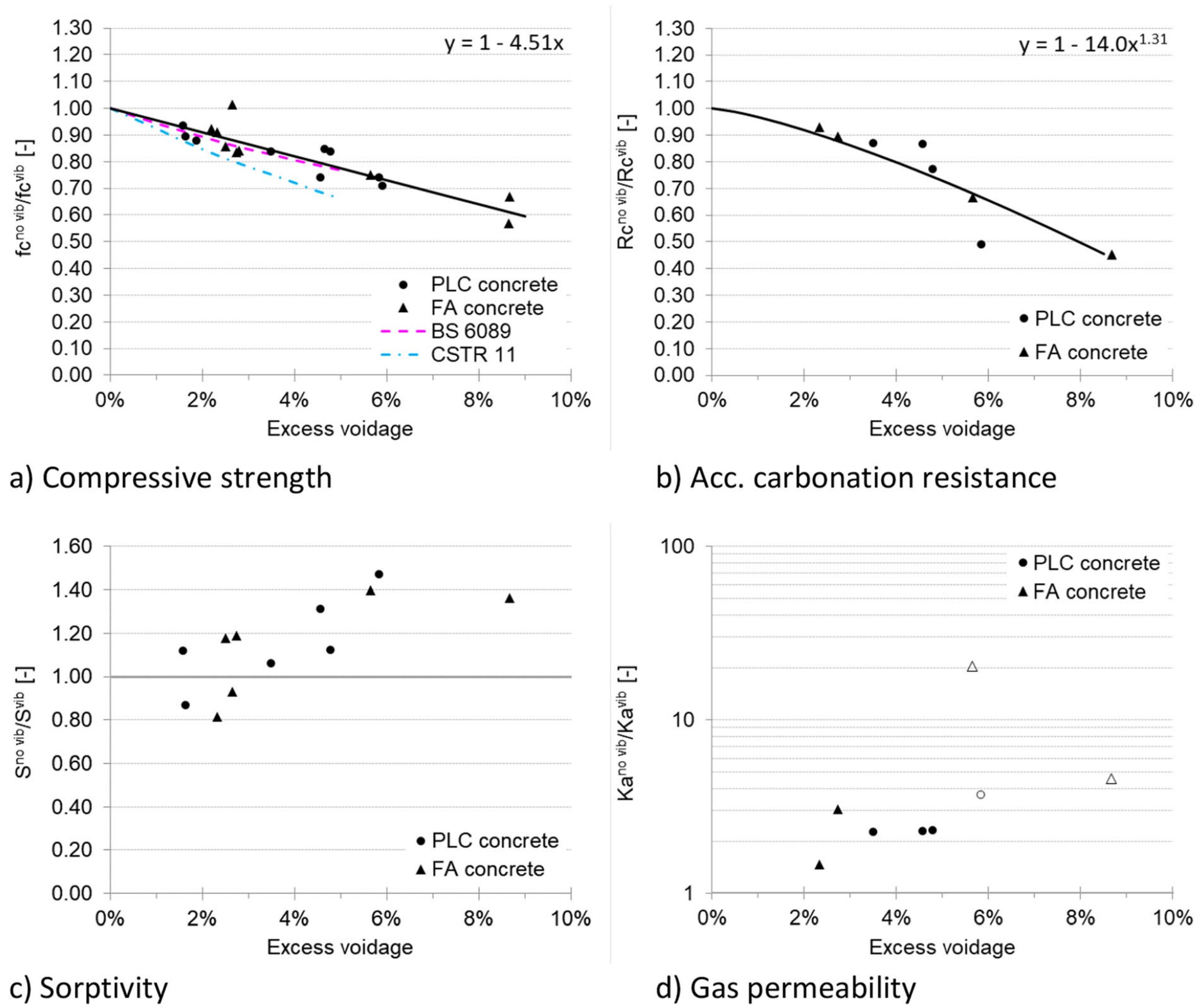

Fig. 7 Relative properties of non-vibrated concrete vs Excess voidage (beams and columns)

from changes in the capillary pore structure (e.g. increase in the volume and average diameter of capillary pores). It could be argued that the cause for the increase in sorptivity is related to the fact that the increase in porosity resulting from poor compaction may amplify the drying rates during the preconditioning of the test specimens, by increasing the concrete permeability and the volume of empty pores available for absorption. However, this does not seem to be the prevailing cause, considering that Gonen and Yazicioglu [4] observed increased sorptivities in poorly compacted concrete specimens dried at 105 °C until constant mass.

Figure 7d shows that the gas permeability also does not show a clear correlation with the excess voidage. This weak correlation may be primarily related to the large scatter of the gas permeability test results, especially for the largest excess voidages, where only a single non-vibrated-concrete specimen could be tested (empty markers in Fig. 7d). The excessively high permeability of the specimens (with non-vibrated concrete) that could not be properly tested (as their permeability were above the reliable range of the permeameter), demonstrates the great sensitivity of the gas permeability test to defects in concrete pore structure, such as those induced by poor compaction.

The weak correlations observed in Fig. 7c and d highlight the limitation of using the water absorption or the gas permeability tests to solve disputes over the quality of the supplied concrete. This is because there

Table 6 Correction factors for compaction as a function of excess voidage

Excess voidage (%)	$C^{fc}_{Comp.}$	$C^{Rc}_{Comp.}$
0.0	1.00	1.00
0.5	1.02	1.01
1.0	1.05	1.03
1.5	1.07	1.06
2.0	1.10	1.09
2.5	1.13	1.12
3.0	1.16	1.16
3.5	1.19	1.20
4.0	1.22	1.25
4.5	1.25	1.31
5.0	1.29	1.37
5.5	1.33	–
6.0	1.37	–
6.5	1.41	–
7.0	1.46	–
7.5	1.51	–
8.0	1.56	–
Standard deviation	0.08	0.05

Fig. 8 Disruptions of the carbonation front due to extremely poor compaction (concrete S0.65F)

are still no tools able to distinguish if the cause of a possible insufficient quality of concrete in the structure (measured by these properties) is attributed to a poor potential quality of concrete or to inadequate execution conditions, such as poor compaction.

4.1.3 Performance properties vs excess of open coarse porosity

Figure 9 shows the excess of open coarse porosity measured in the concrete from beams and columns as a function of the excess voidage. The excess of open coarse porosity shows a high sensitivity to the level of concrete compaction, averaging about half of the excess voidage. However, for concrete close to full compaction (i.e. low excess voidages), fly ash concrete shows excesses of open coarse porosity much lower than the general trend. This may be due to the refinement of concrete pore structure promoted by fly ash reactions [43, 44], which may have reduced its connectivity and, consequently, the overall access of water to pores during the vacuum process.

Overall, fairly good correlations were found between the excess of open coarse porosity and both the compressive strength and the carbonation resistance, as shown in Fig. 10. The following expressions were derived from regression analysis, in the same way as expressions (8) and (9):

$$\frac{f_c^{vib}}{f_c^{novib}} = 1/(1 - 7.83 \times \text{Excess of open coarse porosity}) \tag{10}$$

$$\frac{R_c^{novib}}{R_c^{vib}} = 1/\left(1 - 196 \times \text{Excess of open coarse porosity}^{1.86}\right) \tag{11}$$

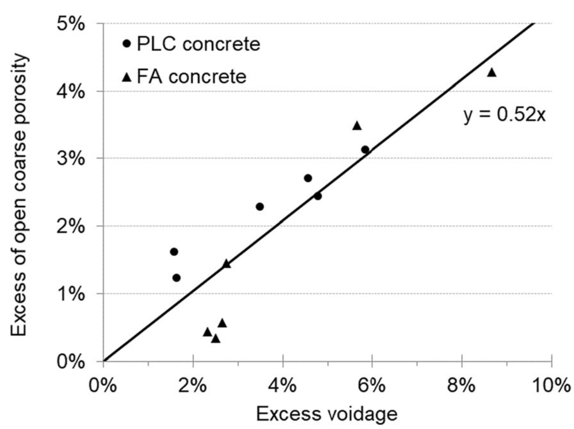

Fig. 9 Excess of open coarse porosity vs Excess voidage (beams and columns)

with standard errors of estimate of 0.07 and 0.05, respectively. Table 7 shows the correction factors for taking into account the effect of compaction on compressive strength and accelerated carbonation resistance, estimated from expressions (10) and (11), respectively.

For the practical application of the excess of open coarse porosity as a compaction indicator in disputes where no information on the fully-compacted concrete is available, further research is still needed to know what typical values of the potential open coarse porosity are expected. For that purpose, tests should be performed on concrete specimens compacted under standard conditions, such as those used in the preparation of control specimens. Once a typical value is found, it should be subtracted from the open coarse porosity measured on the cores when calculating the excess of open coarse porosity of concrete in the structures. Preliminary results could be obtained in standard specimens made with the compositions used in this study. The results showed potential open coarse porosities up to 1.3 vol.% for the Portland concrete (although concrete S0.50 and S0.35 showed values lower than 0.5 vol.%), and up to about 0.3% in the fly ash concrete. Based on these values and on the information given in Table 7, and assuming a general value of about 0.75 vol. %, it may be expected that the uncertainty associated with the potential open coarse porosity should not impact the estimated correction factors $C^{fc}_{Comp.}$ and $C^{Rc}_{Comp.}$ in more than 0.06 and 0.04. This relatively low impact shows the weak dependence of this compaction indicator on the information available on fully-compacted concrete, which should be acceptable in most cases.

Table 7 Correction factors for compaction as a function of excess of open coarse porosity

Excess of open coarse porosity (%)	$C^{fc}_{Comp.}$	$C^{Rc}_{Comp.}$
0.00	1.00	1.00
0.25	1.02	1.00
0.50	1.04	1.01
0.75	1.06	1.02
1.00	1.08	1.04
1.25	1.11	1.06
1.50	1.13	1.09
1.75	1.16	1.12
2.00	1.19	1.16
2.25	1.21	1.20
2.50	1.24	1.26
2.75	1.27	1.32
3.00	1.31	–
3.25	1.34	–
3.50	1.38	–
3.75	1.42	–
4.00	1.46	–
Standard deviation	0.07	0.05

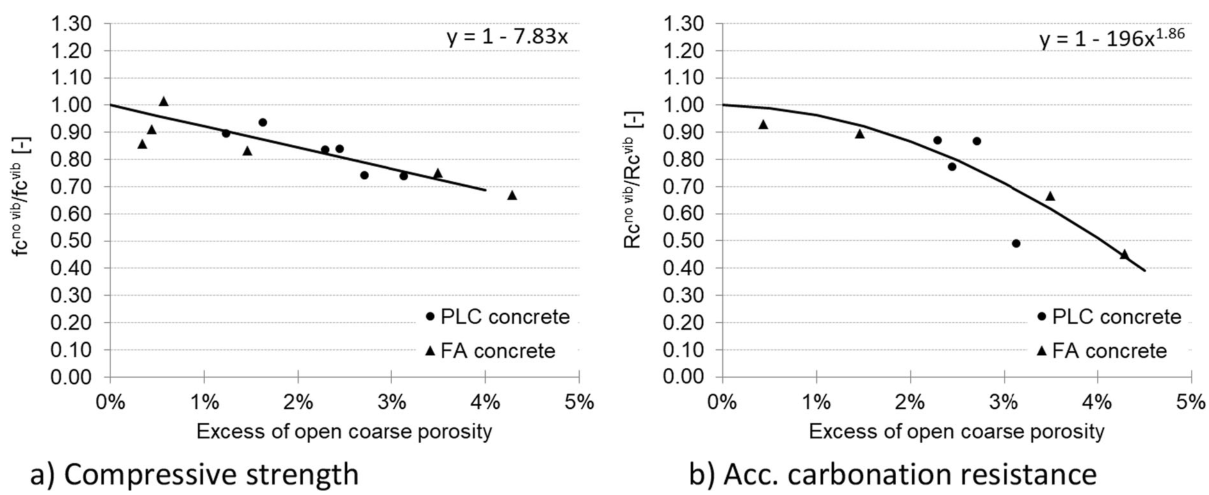

Fig. 10 Relative properties of non-vibrated concrete vs Excess of open coarse porosity (beams and columns)

4.2 Slabs

Figure 11 shows the measured relative properties of non-vibrated concrete from the slabs. Overall, the lack of vibration shows less impact on the concrete quality, resulting in smaller excess voidages compared to beams and columns. This may be due to some compaction induced by the levelling procedure applied on the top surface of non-vibrated slabs and to the fact that the distance the air has to travel inside the slabs to escape from the top surface is very small compared to that inside the beams and columns. However, a distinct behaviour of the concrete from slabs can be observed compared to that from beams and columns. Although the lack of vibration led to excess voidage in the concrete from slabs, greater compressive strengths were generally obtained compared to vibrated concrete (with practically the only exception being the concrete S0.65F, which showed the largest excess voidage of 4.2 vol.%). In fact, no apparent relationship can be observed between the compressive strength and the excess voidage. Despite some attempts (e.g. several cores were horizontally drilled from the slabs to assess the effect of the direction of drilling on concrete strength, but no significant differences were found between the strengths of horizontally and vertically drilled cores), the reasons for such different behaviour remain unknown. Nevertheless, the results obtained in this study suggest that the empirical factors currently used for correcting the compressive strength of concrete on the basis of its excess of porosity, such as those given

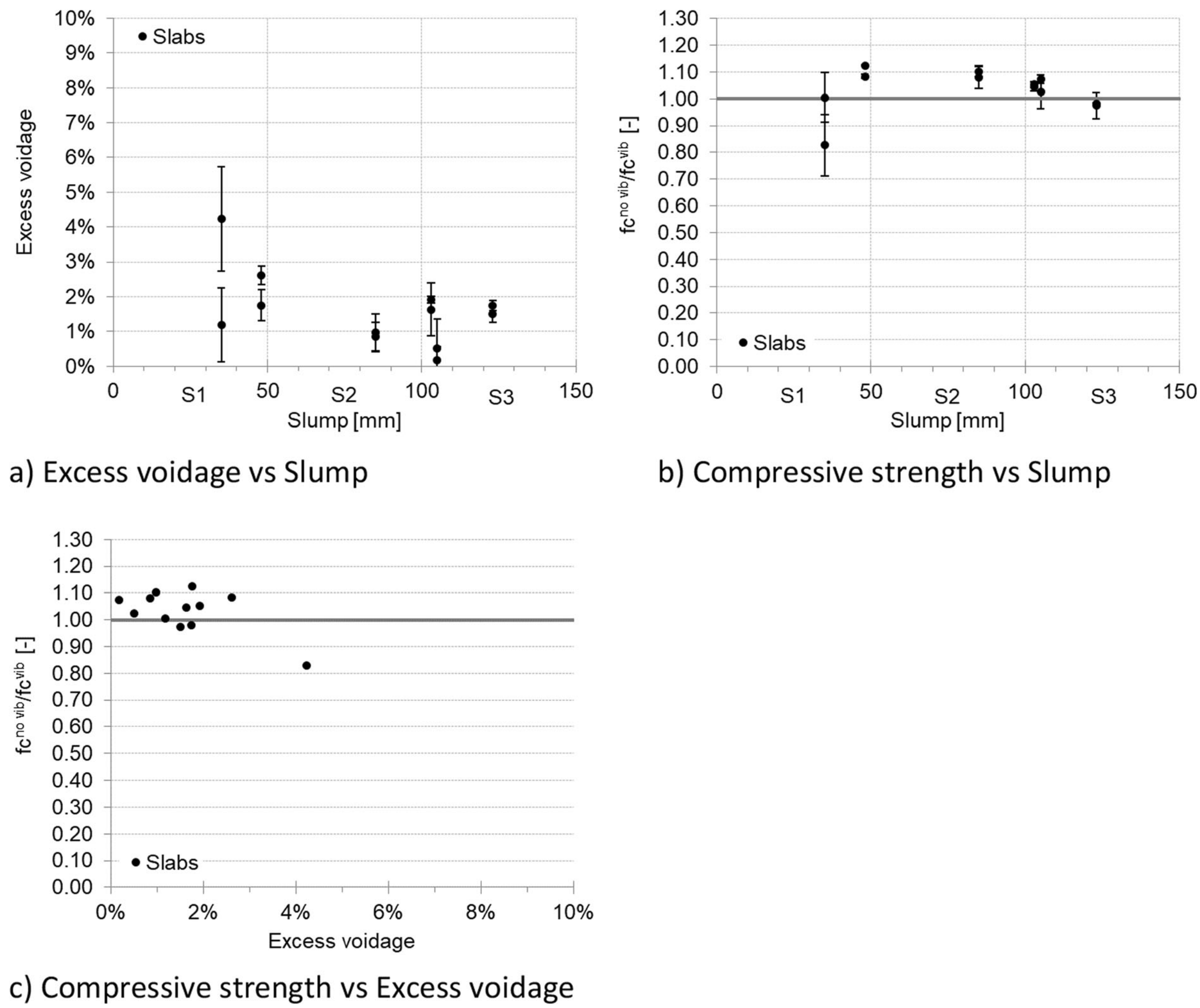

Fig. 11 Relative properties of non-vibrated concrete (slabs)

by CSTR11 [9] and BS 6089 [11], may not be adequate to assess the effects of on-site compaction on the quality of concrete in slabs.

5 Conclusions

Several real-scale concrete elements were produced to study the impact of poor compaction on compressive strength and durability-based properties of concrete with and without fly ash addition. From this study, the following conclusions can be drawn:

a. A promising compaction indicator for concrete was developed on the basis of the open coarse porosity resulting from imperfect compaction. It is determined in an objective manner and shows a weak dependence on the information available on the potential properties of concrete, while exhibiting a good correlation with the loss of compressive strength and carbonation resistance of concrete resulting from poor compaction;
b. New correction factors for compaction applicable in cases of dispute over the compressive strength and carbonation resistance of the supplied concrete were developed on the basis of the excess of the open coarse porosity, as well as of the excess voidage. The results showed that these factors are apparently not affected by concrete mix proportions or incorporation of fly ash;
c. The concrete compressive strength from slabs did not correlate with the excess voidage resulting from poor compaction. This observation suggests that the existing correction factors based exclusively on the excess voidage may not be adequate to assess the impact of compaction on the concrete compressive strength in slabs. However, the causes of such lack of correlation remain unknown;
d. Vibration seems to cease improving the quality of bulk concrete at the upper end of the slump class S3 (i.e. slumps above $\sim$ 140 mm), which suggests that, for greater slumps, concrete should only require vibration in areas close to moulding surfaces, such as those of forms, reinforcement, etc. It also suggests that, in cases of dispute, no correction for compaction should be needed in the estimation of the potential properties of concrete for specified slump classes above S3;
e. The self-weight of fresh concrete only impacts the quality of poorly compacted concrete;
f. Poor compaction increased the sorptivity of concrete (at least up to $\sim$ 9 vol.% of excess voidage), proving that poor compaction does not only lead to the occurrence of large voids in concrete, but also affects its capillary pore structure.

This paper is the first of a collection that is being prepared based on the results from a PhD work [20], where the effect of factors related to curing (e.g. temperature, season of casting, etc.) on concrete quality was also evaluated, including the comparison of concrete properties of real-scale elements cast outdoors with those of standard control specimens.

Funding This research was carried out within the PhD studentship SFRH/BD/68603/2010 given to the first author by the Portuguese Foundation for Science and Technology (FCT). Open access funding provided by FCT|FCCN (b-on).

Declarations

Conflict of interest The authors have no conflicts of interest to declare that are relevant to the content of this article.

References

1. Kaplan MF (1960) Effects of incomplete consolidation on compressive and flexural strength, ultrasonic pulse velocity, and dynamic modulus of elasticity of concrete. J Proc 56:853–868. https://doi.org/10.14359/8124
2. Gonçalves A (1987) Resistência do betão nas estruturas. PhD Thesis, LNEC
3. Grampeix G (2012) Effect of internal vibration and concrete rheology on properties of reinforced concrete. In: Proceedings of the 9th fib International PhD Symposium in Civil Engineering. KIT Scientific Publishing, Karlsruhe, pp 387–392

4. Gonen T, Yazicioglu S (2007) The influence of compaction pores on sorptivity and carbonation of concrete. Constr Build Mater 21:1040–1045. https://doi.org/10.1016/j.conbuildmat.2006.02.010
5. Neves R, Santos J, Monteiro A (2011) Estudo sobre a influência da compactação na resistência do betão à carbonatação. In: 6° Congresso Luso - Moçambicano de Engenharia. Maputo
6. Chidiac SE, Maadani O, Razaqpur AG, Mailvaganam NP (2003) Correlation of rheological properties to durability and strength of hardened concrete. J Mater Civ Eng 15:391–399. https://doi.org/10.1061/(ASCE)0899-1561(2003)15:4(391)
7. Gao X, Zhang J, Su Y (2019) Influence of vibration-induced segregation on mechanical property and chloride ion permeability of concrete with variable rheological performance. Constr Build Mater 194:32–41. https://doi.org/10.1016/j.conbuildmat.2018.11.019
8. Chan Y-W, Chen Y-G, Liu Y-S (2003) Effect of consolidation on bond of reinforcement in concrete of different workabilities. Mater J 100:294–301. https://doi.org/10.14359/12667
9. Concrete Society (1987) Technical Report 11. Concrete core testing for strength. The Concrete Society, Camberley
10. EN 13791 (2019) Assessment of in-situ compressive strength in structures and precast concrete components. CEN
11. BS 6089 (2010) Assessment of in-situ compressive strength in structures and precast concrete components – Complementary guidance to that given in BS EN 13791. BSI
12. Beushausen H, Alexander MG, Basheer M et al (2016) Principles of the performance-based approach for concrete durability. In: Beushausen H, Fernandez Luco L (eds) Performance-based specifications and control of concrete durability: state-of-the-art report RILEM TC 230-PSC. Springer, Netherlands, pp 107–131
13. fib Bulletin 66 (2012) Model Code 2010. Final Draft. fib
14. ISO 16204:2012 (2012) Durability — Service life design of concrete structures. ISO
15. LNEC E 465 (2007) Betões. Metodologia para estimar as propriedades de desempenho do betão que permitem satisfazer a vida útil de projecto de estruturas de betão armado ou pré-esforçado sob as exposições ambientais XC e XS. LNEC
16. EHE-08 (2008) Instrucción de hormigón estructural. Real Decreto 1247/2008
17. EN 197-1 (2011) Cement - Part 1: Composition, specifications and conformity criteria for common cements. CEN
18. ACI 309R-05 (2005) Guide for consolidation of concrete. ACI
19. EN 13670 (2009) Execution of concrete structures. CEN
20. Monteiro A (2016) Actual durability-related properties of concrete. PhD Thesis, Instituto Superior Técnico, Universidade de Lisboa & Université Toulouse III - Paul Sabatier
21. EN 12504-1:2009 (2009) Testing concrete in structures - Part 1: Cored specimens - Taking, examining and testing in compression. CEN
22. RILEM TC 56-MHM (1988) CPC-18 Measurement of hardened concrete carbonation depth. Mater Struct 2:453–455
23. RILEM TC 116-PCD (1999) Tests for gas permeability of concrete. Mater Struct 32:174–179
24. EN 12390-7 (2009) Testing hardened concrete – Part 7: Density of hardened concrete. CEN
25. ACI 309.1R-08 (2008) Report on behavior of fresh concrete during vibration. ACI
26. Roussel N, Coussot P (2005) ''Fifty-cent rheometer'' for yield stress measurements: from slump to spreading flow. J Rheol. https://doi.org/10.1122/1.1879041
27. Leemann A, Winnefeld F (2007) The effect of viscosity modifying agents on mortar and concrete. Cem Concr Compos 29:341–349. https://doi.org/10.1016/j.cemconcomp.2007.01.004
28. Lachemi M, Hossain KMA, Lambros V et al (2004) Performance of new viscosity modifying admixtures in enhancing the rheological properties of cement paste. Cem Concr Res 34:185–193. https://doi.org/10.1016/S0008-8846(03)00233-3
29. Khayat K, Guizani Z (1997) Use of viscosity-modifying admixture to enhance stability of fluid concrete. ACI Mater J 94:332–339. https://doi.org/10.14359/317
30. Han D, Lee G-C, Yoon S-J, Kim K-M (2015) Viscosity influence on rising behavior of model air bubbles in fresh mortar. Constr Build Mater 76:10–15. https://doi.org/10.1016/j.conbuildmat.2014.11.016
31. Hasselman D (1963) Relation between effects of porosity on strength and on Young's modulus of elasticity of polycrystalline materials. J Am Ceram Soc 46:564–565
32. Ryshkewitch E (1953) Compression strength of porous sintered alumina and zirconia. J Am Ceram Soc 36:65–68. https://doi.org/10.1111/j.1151-2916.1953.tb12837.x
33. Schiller K (1958) Porosity and strength of brittle solids. Mechanical properties of non-metallic brittle materials. Butterworths Press, London, pp 35–49
34. Balshin M (1949) Relation of mechanical properties of powder metals and their porosity and the ultimate properties of porous metal-ceramic materials. Dokl Akad Nauk SSSR 67:831–834
35. Rößler M, Odler I (1985) Investigations on the relationship between porosity, structure and strength of hydrated Portland cement pastes I. Effect of porosity. Cem Concr Res 15:320–330. https://doi.org/10.1016/0008-8846(85)90044-4
36. Atzeni C, Massidda L, Sanna (1987) Effect of pore size distribution on strength of hardened cement pastes. Paris, pp 195–202
37. Kumar R, Bhattacharjee B (2003) Porosity, pore size distribution and in situ strength of concrete. Cem Concr Res 33:155–164. https://doi.org/10.1016/S0008-8846(02)00942-0
38. Walker S, Bloem D (1955) Design and control of air-entraining concrete. National Ready Mixed Concrete Association, Washington
39. Erkkilä A-L, Leppänen T, Virkajärvi J et al (2021) Quasi-brittle porous material: simulated effect of stochastic air void structure on compressive strength. Cem Concr Res 139:106255. https://doi.org/10.1016/j.cemconres.2020.106255
40. Leemann A, Münch B, Gasser P, Holzer L (2006) Influence of compaction on the interfacial transition zone and the

permeability of concrete. Cem Concr Res 36:1425–1433. https://doi.org/10.1016/j.cemconres.2006.02.010
41. Goodwin F (2006) Chapter 21: volume change. In: Lamond J, Pielert J (eds) Significance of tests and properties of concrete and concrete-making materials STP 169D. ASTM International, Denver
42. Duratinet (2012) Concrete structures - Part IV: testing techniques. In: Maintenance and repair of transport infrastructure: Technical guide. LNEC, p 88
43. Hooton R (1986) Permeability and pore structure of cement pastes containing fly ash, slag and silica fume. ASTM, Denver
44. Malhotra VM (1993) Fly ash, slag, silica fume, and rice husk ash in concrete: A Review. Concr Int 15(4):23–28